

# Na<sub>0.5</sub>K<sub>0.5</sub>NbO<sub>3</sub>–BiFeO<sub>3</sub> lead-free piezoelectric ceramics

Ruzhong Zuo\*, Chun Ye, Xusheng Fang

*School of Materials Science and Engineering, Hefei University of Technology, Tunxi Road 193, Hefei 230009, China*

Received 16 May 2007; received in revised form 16 August 2007; accepted 30 August 2007

## Abstract

Lead-free (Na<sub>0.5</sub>K<sub>0.5</sub>)NbO<sub>3</sub>-based piezoelectric ceramics were successfully fabricated by substituting with a small amount of BiFeO<sub>3</sub> (BF). Difficulty in sintering of pure NKN ceramics can be eased by adding a few molar percent of BF, and the crystalline structure is also changed, leading to a morphotropic phase boundary (MPB) between ferroelectric orthorhombic and rhombohedral phases. The MPB exists near the 1–2 mol% BF-substituted NKN compositions, exhibiting enhanced ferroelectric, piezoelectric, and electromechanical properties of  $P_r = 23.3 \mu\text{C}/\text{cm}^2$ ,  $d_{33} = 185 \text{ pC}/\text{N}$ , and  $k_p = 46\%$ , compared to an ordinarily sintered pure NKN ceramics. The MPB composition has a Curie temperature of  $\sim 370^\circ\text{C}$ , comparable to that of some commercial PZT materials.

© 2007 Elsevier Ltd. All rights reserved.

*Keywords:* A. Ceramics; D. Ferroelectricity; D. Microstructure; D. Piezoelectricity

## 1. Introduction

An increasing attention has been paid to lead free or lead content reduced piezoelectric ceramics in recent years. A common knowledge is that lead will have brought a great threat to the environment. The traditional piezoelectric ceramics or single crystals are mostly Pb-based perovskite materials where lead oxide takes at least 70 wt% of the total [1]. In the last few years, Na<sub>0.5</sub>K<sub>0.5</sub>NbO<sub>3</sub> (NKN)-based compositions with a morphotropic phase boundary (MPB) have shown greater advantages over another typical lead-free piezoelectric candidate material system, (Bi<sub>0.5</sub>Na<sub>0.5</sub>)TiO<sub>3</sub> (BNT)-based MPB materials, such as higher Curie temperatures ( $T_c$ ) up to nearly  $400^\circ\text{C}$ , better piezoelectric and electromechanical properties, and so on. NKN ceramics have two-phase transition temperatures above room temperature, one from orthorhombic to tetragonal at  $\sim 200^\circ\text{C}$  and another from tetragonal to cubic at  $T_c$  ( $\sim 420^\circ\text{C}$ ). An ordinarily sintered NKN ceramics [2] may have electrical properties of the piezoelectric constant,  $d_{33} \sim 80 \text{ pC}/\text{N}$ ; the planar electromechanical coupling factor,  $k_p \sim 36\text{--}40\%$ ; the mechanical quality factor,  $Q_m \sim 130$ ; and the room temperature dielectric

constant,  $\epsilon_{33}^T/\epsilon_0 \sim 290$ . However, the hot pressed NKN ceramics [3] have been reported to possess a much larger  $d_{33}$  up to  $160 \text{ pC}/\text{N}$  and a  $k_p$  of  $\sim 45\%$ . This is because NKN compositions are rather difficult to densify by an ordinary sintering technique. Other than pressure-assisted sintering [3–6], many other routes such as sintering aids [7–10], control of stoichiometry [11,12], alkaline- or rare-earth elements doping [11,13–15], solid solutions [16–18] with ATiO<sub>3</sub> (A: Ca, Sr, or Ba), and so on, have been utilized to improve their densification. Furthermore, their properties can be significantly enhanced by doping a small amount of Li, Ta, Sb, etc., due to a MPB between ferroelectric orthorhombic and tetragonal phases [19–23]. The textured (Li, Ta, Sb)-doped NKN ceramics [20] were reported to possess comparable piezoelectric properties to a hard PZT. However, this system is distinguished from PZT systems whose MPB lies between ferroelectric rhombohedral and tetragonal phases [1]. The MPB is of importance for high-performance piezoelectric materials, since a nearly continuous rotation of spontaneous polarization vectors under the external electric field can be realized for MPB compositions [24–28], inducing a superior piezoelectric activity.

Bismuth ferrite, BiFeO<sub>3</sub> (BF), has been known as a multiferroic material with a rhombohedral perovskite structure at room temperature. It has high phase transition

\*Corresponding author. Tel.: +86 551 2905285.

E-mail address: [piezolab@hfut.edu.cn](mailto:piezolab@hfut.edu.cn) (R. Zuo).

temperatures (i.e., Curie temperature  $\sim 810^\circ\text{C}$  and Néel temperature  $\sim 384^\circ\text{C}$ ) [29,30]. It can be made in both ceramic and thin film forms for electromagnetic or piezoelectric applications. As far as the piezoelectric application is concerned, it forms a MPB solid solution ceramic with  $\text{PbTiO}_3$ , which was considered to be a promising piezoelectric material for high-temperature application [31,32]. However, this system has a large current leakage and a high coercive electric field, both of which make it difficult to become a good piezoelectric by a conventional poling process [33,34]. These problems have been eased by many attempts, such as doping a few molar percent of La, Ga, and so on [35], or carefully controlling sintering conditions [36–38]. BF was also used to improve the piezoelectric properties of BNT ceramics [39].

In this study, a small amount of BF was used to partially substitute NKN. The influence of BF addition on the sinterability, phase transitions, electrical properties of NKN ceramics was investigated. A new MPB was identified by a series of X-ray diffraction (XRD) data and dielectric property measurement. Electrical characterization was carried out only for the compositions near the MPB.

## 2. Experimental

$(1-x)\text{NKN}-x\text{BF}$  ceramics ( $x = 0, 0.005, 0.01, 0.02, 0.03, 0.05, 0.10$ ) were synthesized by means of a conventional mixed oxide route. High-purity oxides and carbonates,  $\text{Nb}_2\text{O}_5$  (99.9%),  $\text{Bi}_2\text{O}_3$  (99.97%),  $\text{Fe}_2\text{O}_3$  (99.5%) and  $\text{Na}_2\text{CO}_3$  (99.5%),  $\text{K}_2\text{CO}_3$  (99.0%), were used as starting materials which had been treated carefully by a special drying process before use, particularly for sodium/potassium carbonates. These powders were placed in an oven at  $120^\circ\text{C}$  for 2 days and then stored in a moisture-free vessel. The weighed powders were mixed by a planetary ball mill in an anhydrous alcohol for 12 h. After drying, the calcination was carried out at temperatures from  $850$  to  $900^\circ\text{C}$  for 5 h according to the compositions in a covered alumina crucible. The calcined powders were ground in an agate mortar and then calcined once again in order to improve compositional distribution. The well-calcined powders were ball milled as above for 24 h and sieved through 230 meshes.

The disk specimens compacted in a stainless die under a uniaxial pressure of 50 MPa were sintered in air in the temperature range of  $1000$ – $1130^\circ\text{C}$  for 3 h, depending on the compositions. A platinum foil was placed under the samples covered with an inverted alumina crucible to reduce the reaction between the samples and the alumina substrate and also to prevent the volatilization of potassium. This proved to be necessary in modifying the densification of NKN-based materials [7].

Densities of the samples sintered at different temperatures were measured by the Archimedes method. The microstructure was observed by a scanning electron microscope (SEM, Philips Electronic Instruments). Powder

XRD (Rigaku) was utilized to identify the crystal structures and the phase content of each composition.

For the electrical characterization, all samples were treated by a careful polishing process to get parallel scratch-free surfaces. Silver paste was fired on two sides of each specimen as electrodes. Dielectric properties as a function of temperature and frequency were measured by an impedance analyzer (HP 4284). Polarization versus electric field hysteresis loops were measured in a silicone oil bath by applying an electric field of triangular waveform at a frequency of 50 mHz by means of a modified Sawyer–Tower bridge. The measurement of piezoelectric and electromechanical properties was carried out only 24 h after a poling process. The applied poling fields were slightly changed according to the compositions, ranging from 1.5 to 3 kV/mm. The poling treatment was carried out in a silicone oil bath with a programmable temperature controller. The poling temperature varied from  $50$  to  $100^\circ\text{C}$ , considering the composition and the conductivity of each specimen.

## 3. Results and discussion

The XRD patterns of  $(1-x)\text{NKN}-x\text{BF}$  compositions composed at  $1050^\circ\text{C}$  for 2 h are shown in Fig. 1. All compositions have pure perovskite structures, yet showing a changing symmetry with increasing the BF content. When  $x = 0$ , the material displays a typical orthorhombic symmetry at room temperature, as reported for the MPB NKN composition [40]. However, the structure changes rapidly with the addition of BF. When  $0.01 < x \leq 0.03$ , it becomes a rhombohedral perovskite structure; with further increasing BF content, it becomes cubic within the studied composition range. The split (200) peaks from an orthorhombic symmetry are gradually combined into a single peak of a rhombohedral structure as  $x$  increases.

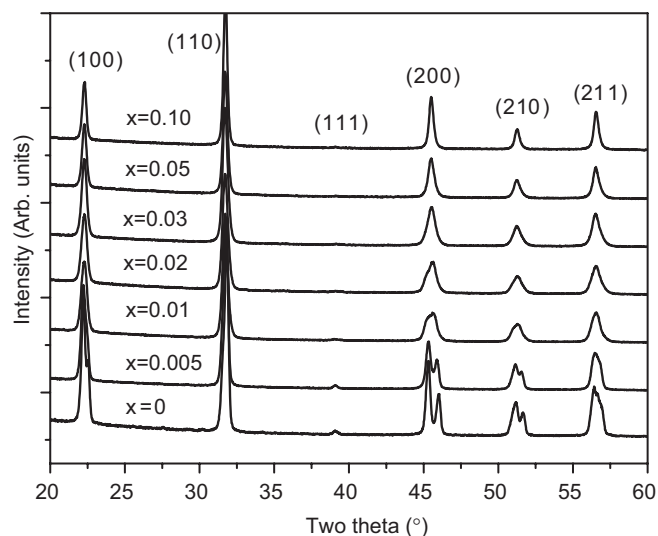


Fig. 1. X-ray diffraction patterns of  $(1-x)\text{NKN}-x\text{BF}$  ceramics.

The transitional point for the structure change can be identified to be near  $x = 0.01$ . Therefore, an MPB between orthorhombic and rhombohedral structures can be expected in this system. Although the peak splitting of such reflections as (1 1 1) or (2 1 0) for a rhombohedral structure

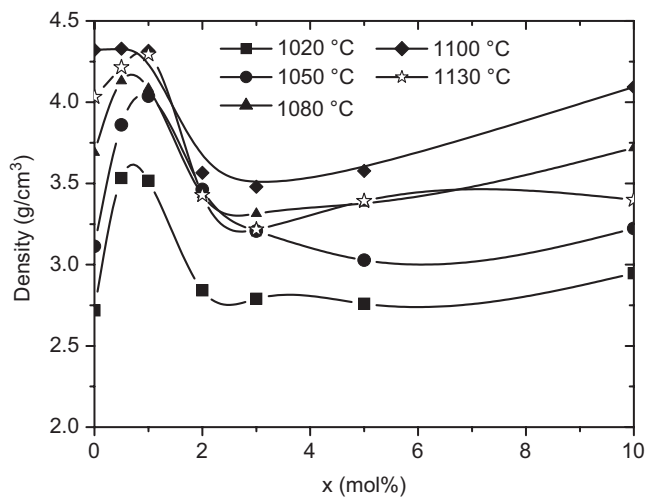


Fig. 2. Sintering profiles of  $(1-x)\text{NKN}-x\text{BF}$  ceramics sintered by holding samples at different temperatures for 3 h.

is not detectable in Fig. 1, so that a doubt of whether the structure changes from orthorhombic phases to rhombohedral or cubic phases may occur, an easy way to clarify this point can be obtained from the measurement of dielectric and piezoelectric properties.

Moreover, the addition of a small amount of BF also influences the densification behavior of NKN ceramics, as shown in Fig. 2. It is a fact that a pure NKN composition is difficult to become highly dense by ordinary sintering. Samples with different  $x$  were sintered at different temperatures for 3 h. The densities were measured, plotted as a function of the BF content  $x$  and temperature. On one hand, with increasing the sintering temperature, most compositions show improved densification; however, the densities start to decrease when the temperature reaches 1130 °C. This can be caused by the volatilization of potassium and sodium and the grain growth at high temperature. The grain coarsening tends to decrease the sintering potential of the materials. On the other hand, the samples show good sintering behavior when doped with only a small amount of BF. More BF-added NKN solid solution ceramics may have relatively high sintering temperature. This point is of value to its application, because the MPB was found approximately at  $x = 0.01$ . Although the optimal temperature for each composition was different, only samples with densities of more

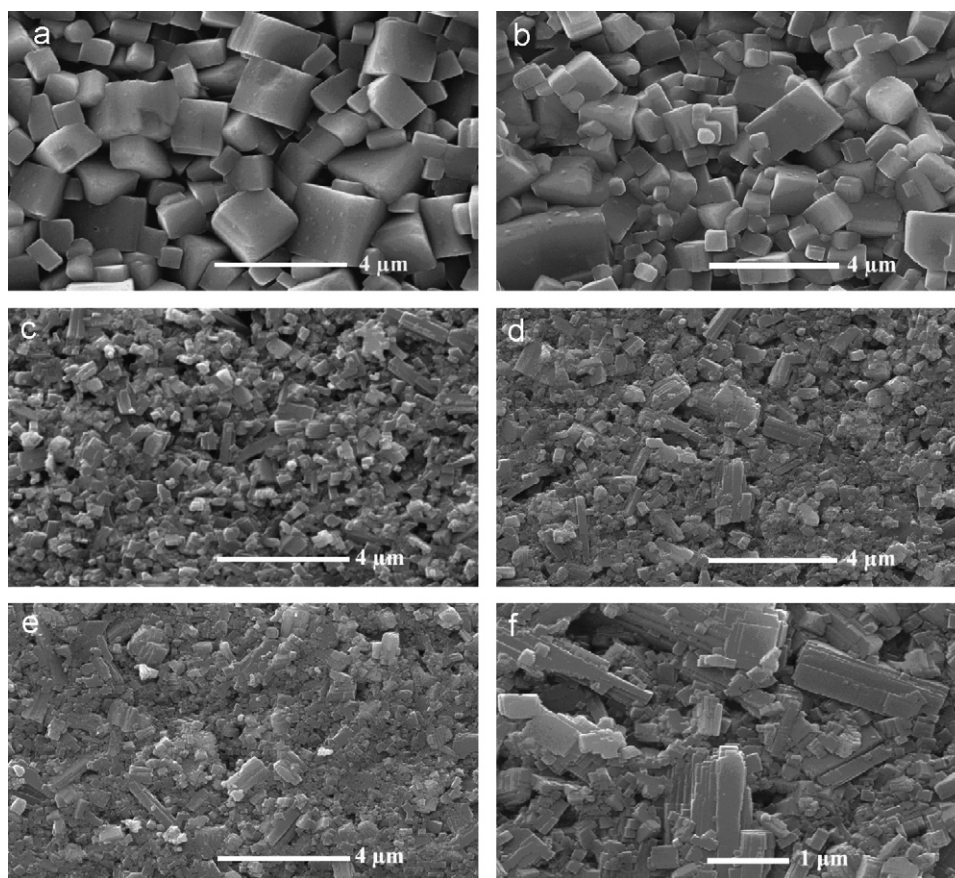


Fig. 3. Morphology of  $(1-x)\text{NKN}-x\text{BF}$  ceramics sintered at 1100 °C for 3 h: (a)  $x = 0$ , (b)  $x = 0.01$ , (c)  $x = 0.02$ , (d)  $x = 0.03$ , (e)  $x = 0.05$ , and (f) high magnification for the sample with  $x = 0.03$ .

than 96% theoretical values were used for electrical characterization.

The microstructure of different compositions sintered at 1100 °C is compared in Fig. 3. It is noticeable that the grain size changes with varying the BF content. An extremely evident change takes place at  $x = 0.01$ – $0.02$ . When  $x = 0.01$ , the grain size is  $\sim 2\mu\text{m}$  in average; it decreases to  $\sim 0.6\mu\text{m}$  for the sample with  $x = 0.02$ . We cannot catch what role the BF plays in influencing the grain growth; however, one can take note of that not only the grain size, but also the grain morphology was changed. The change in grain size seems to be finished by disintegration of big grains into small ones, as seen from Fig. 3(f). Noticeably, a dense NKN ceramic is milk-white and changes its color when immersed in water for a long time, accompanied by an increasing conductivity (loss). We think that this is due to so-called deliquescence process based on a reaction between  $\text{H}_2\text{O}$  molecule and potassium/sodium containing second phases at the grain boundary of bulk NKN ceramics. However, this feature was significantly improved by a small amount of BF substitution. The BF-substituted NKN ceramic exhibits light red color and gets redder with increasing the BF content. It shows much less deliquescence in water, but may display higher leakage current when BF content is more. It should be noted that the improved deliquescence characteristic will lead to the enhanced sinterability. Moreover, a small amount of BF could act as impurities in the NKN composition, thus promoting the densification.

Fig. 4 shows the dielectric constant and dissipation factor of  $(1-x)\text{NKN}-x\text{BF}$  ceramics as a function of temperature. When  $x = 0$ , the material shows two-phase transition temperatures, corresponding to the ferroelectric orthorhombic–tetragonal transition at  $\sim 200^\circ\text{C}$ , and the tetragonal–cubic transition at  $\sim 420^\circ\text{C}$ , as reported for pure NKN ceramics [7]. With increasing the BF content, both of these phase transition temperatures shift to low temperatures. When  $x = 0.02$ , the orthorhombic–tetragonal phase transition disappears and the material becomes a solely rhombohedral structure and has a Curie temperature of  $\sim 330^\circ\text{C}$ . This result confirms that the compositions with  $0.01 < x \leq 0.03$  are rhombohedral ferroelectrics, not cubic paraelectrics. For samples with  $x > 0.05$ , no peaks in dielectric constant versus temperature curves can be observed, probably because the peaks are shifted below room temperature. These results are consistent with XRD analysis. Moreover, it is noticeable that the rhombohedral ferroelectric compositions show much lower peak dielectric constants and broad phase transitions, compared to orthorhombic ferroelectric compositions. Such behavior can originate from more complex occupation of the A and B sites in an  $\text{ABO}_3$  perovskite structure and the fine grain size in these compositions. One can also note that the dielectric loss changes significantly with increasing  $x$ . When  $x$  is below 0.01,  $(1-x)\text{NKN}-x\text{BF}$  ceramics display decreased dielectric losses of as low as 4%, probably due to their improved densities. However, the loss values

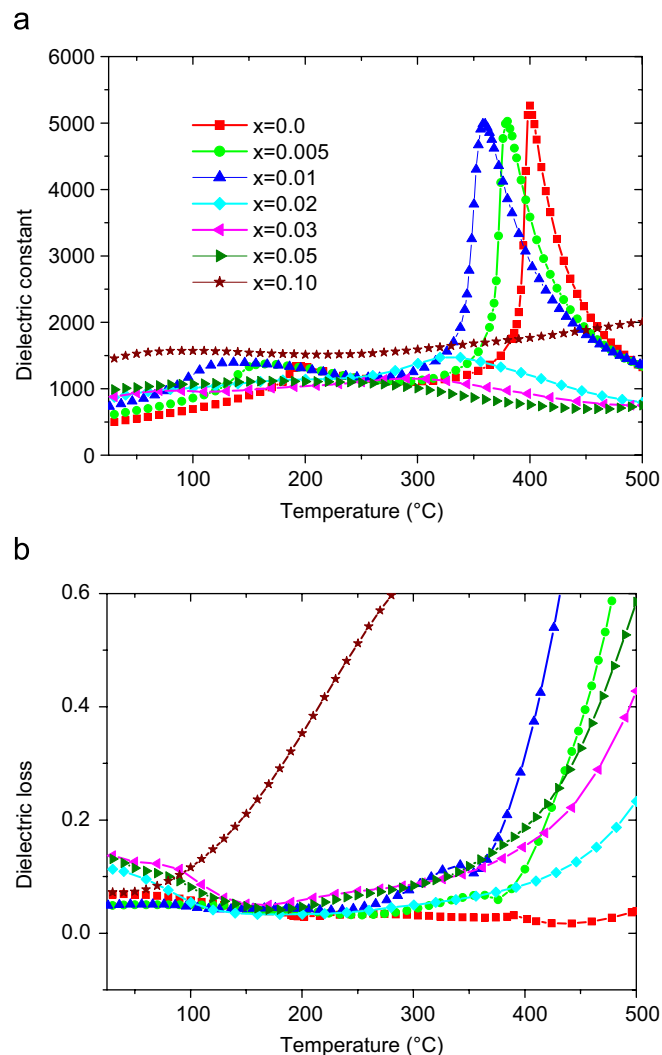


Fig. 4. Dielectric constant (a) and loss (b) of  $(1-x)\text{NKN}-x\text{BF}$  ceramic samples at 100 kHz as a function of temperature.

increase dramatically when  $x$  is above 0.02. It reaches 14% at room temperature for 3 mol% BF-substituted NKN ceramics. As we know, BF intrinsically has a large leakage current. Therefore, the addition of BF into NKN ceramics may cause the conductivity problems.

A comparison of polarization versus electric field curves for pure NKN ceramics and 1 mol% BF-substituted NKN ceramics is made in Fig. 5. It can be seen that 1 mol% BF substitution significantly enhances the ferroelectricity of NKN compositions. For pure NKN ceramics, the remnant polarization  $P_r$  and the coercive electric field  $E_c$  are  $13.6\mu\text{C}/\text{cm}^2$  and  $990\text{V}/\text{mm}$ , respectively; however, both of values change to  $23.3\mu\text{C}/\text{cm}^2$  and  $870\text{V}/\text{mm}$ , respectively, after 1 mol% BF is added. The enhancement of densification due to the BF addition may be one of the reasons. A small reduction of the coercive field means that the domain mobility gets larger after BF substitution.

Fig. 6 shows the piezoelectric and electromechanical properties of  $(1-x)\text{NKN}-x\text{BF}$  ceramics ( $0 \leq x \leq 0.05$ ) as a function of the BF concentration. Around the MPB, the

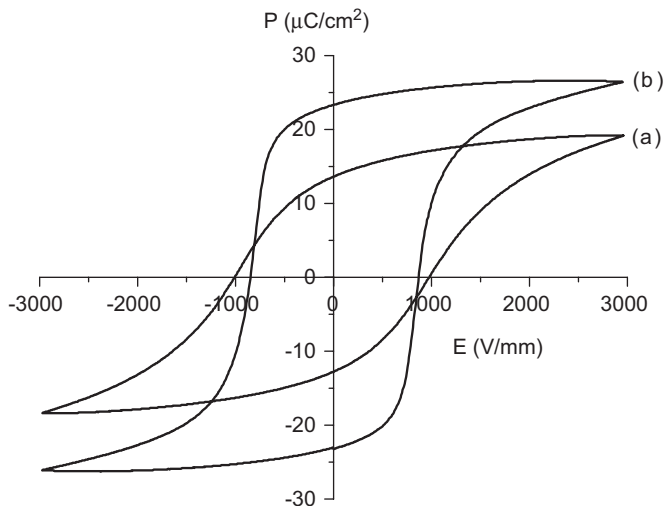


Fig. 5. Polarization versus electric field curves at 50mHz for (a) pure NKN ceramic and (b) 1 mol% BF-substituted NKN ceramic sintered at 1100 °C for 3 h.

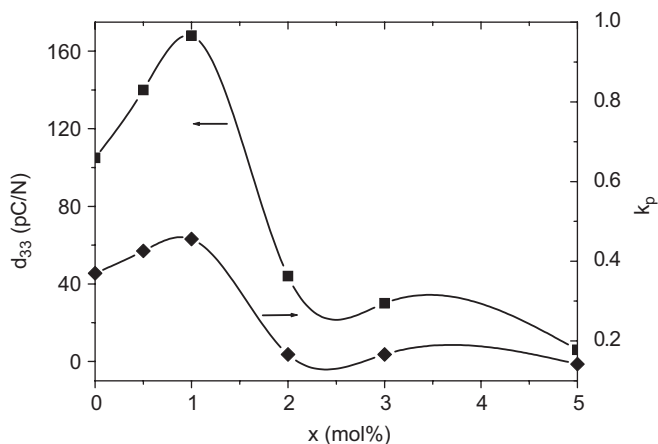


Fig. 6. Piezoelectric and electromechanical properties of  $(1-x)\text{NKN}-x\text{BF}$  ceramics as a function of the BF content  $x$ .

materials show a strong composition dependence of the electrical properties. The best piezoelectric and electromechanical properties of  $d_{33} = 185 \text{ pC/N}$  and  $k_p = 46\%$  appear in the composition of  $0.99\text{NKN}-0.01\text{BF}$ , regardless of continuing decrease in grain size. For pure NKN ceramic, it has a  $d_{33}$  of  $105 \text{ pC/N}$  and a  $k_p$  of  $37\%$ . The addition of a small amount of BF evidently enhances the piezoelectric activities of solid solution ceramics till the peak values are reached nearly the MPB. Above this boundary, the properties decrease rapidly with adding more BF into NKN ceramics. Therefore, two roles can be expected from the BF substitution. One is that a small amount of BF tends to improve the sinterability of NKN ceramics, as we discussed above. Another is that the MPB between ferroelectric orthorhombic and rhombohedral phases is formed due to the addition of BF. The second is well known to play a more important role in the enhancement of piezoelectric properties.

#### 4. Conclusions

$(1-x)\text{NKN}-x\text{BF}$  solid solution ceramics were successfully fabricated by an ordinary sintering technique. The MPB between ferroelectric orthorhombic and rhombohedral phases exists near the 1–2 mol% BF-substituted NKN compositions. In addition, the addition of BF also promotes the sintering of NKN ceramics, inhibits the grain growth, improves the deliquescence characteristic, and enhances the ferroelectricity. The  $0.99\text{NKN}-0.01\text{BF}$  ceramics near the MPB possess best properties of  $P_r = 23.3 \mu\text{C/cm}^2$ ,  $d_{33} = 185 \text{ pC/N}$ , and  $k_p = 46\%$  in all compositions.

#### Acknowledgments

This work was financially supported by HFUT RenCai Foundation (No. 103-035006) and a special Program for Excellence Selection “R&D of Novel Lead Free Piezoelectric Ceramics” (No. 103-035034).

#### References

- [1] B. Jaffe, W.R. Cook, H. Jaffe, *Piezoelectric Ceramics*, Academic Press, New York, 1971.
- [2] L. Egerton, D.M. Dillon, *J. Am. Ceram. Soc.* 42 (1959) 438.
- [3] G.H. Haertling, *J. Am. Ceram. Soc.* 50 (1967) 329.
- [4] L. Egerton, C.A. Bieling, *Ceram. Bull.* 47 (1968) 1151.
- [5] R.E. Jaeger, L. Egerton, *J. Am. Ceram. Soc.* 45 (1962) 209.
- [6] J.F. Li, K. Wang, B.P. Zhang, L.M. Zhang, *J. Am. Ceram. Soc.* 89 (2006) 706.
- [7] R.Z. Zuo, J. Rodel, R.Z. Chen, L.T. Li, *J. Am. Ceram. Soc.* 89 (2006) 2010.
- [8] S.H. Park, C.W. Ahn, S. Nahm, J.S. Song, *Jpn. J. Appl. Phys.* 43 (2004) L1072.
- [9] C.W. Ahn, H.C. Song, S. Nahm, S.H. Park, K. Uchino, S. Priya, H.G. Lee, N.K. Kang, *Jpn. J. Appl. Phys.* 44 (2005) L1361.
- [10] M. Matsubara, T. Yamaguchi, K. Kikuta, S. Hirano, *Jpn. J. Appl. Phys.* 43 (2004) 7159.
- [11] Z.S. Ahn, W.A. Schulze, *J. Am. Ceram. Soc.* 70 (1987) C–18.
- [12] J. Yoo, K. Lee, K. Chung, S. Lee, K. Kim, J. Hong, S. Ryu, C. Lhee, *Jpn. J. Appl. Phys.* 45 (2006) 7444.
- [13] B. Malic, J. Bernard, J. Holc, D. Jenko, M. Kosec, *J. Eur. Ceram. Soc.* 25 (2005) 2707.
- [14] S.N. Murty, K. Umarantham, A. Bhanamathi, *Ferroelectrics* 82 (1988) 141.
- [15] M. Kosec, D. Kolar, *Mater. Res. Bull.* 10 (1975) 335.
- [16] Y.F. Chang, Z.P. Yang, L.L. Wei, B. Liu, *Mater. Sci. Eng. A* 437 (2006) 301.
- [17] M. Kosec, V. Bobnar, M. Hrovat, J. Bernard, B. Malic, J. Holc, *J. Mater. Res.* 19 (2004) 1849.
- [18] Y. Guo, K. Kakimoto, H. Ohsato, *Jpn. J. Appl. Phys.* 43 (2004) 6662.
- [19] Y. Guo, K. Kakimoto, H. Ohsato, *Appl. Phys. Lett.* 85 (2004) 4121.
- [20] Y. Saito, H. Takao, T. Tani, T. Nonoyama, K. Takatori, T. Homma, T. Nagaya, M. Nakamura, *Nature* 432 (2004) 84.
- [21] E. Hollenstein, M. Davis, D. Damjanovic, N. Setter, *Appl. Phys. Lett.* 87 (2005) 182905.
- [22] M. Matubara, T. Yamaguchi, W. Sakamoto, K. Kikuta, T. Yogo, S. Hirano, *J. Am. Ceram. Soc.* 88 (2005) 1190.
- [23] S.J. Zhang, R. Xia, T.R. Shrout, G.Z. Zang, J.F. Wang, *J. Appl. Phys.* 100 (2006) 104108.
- [24] H. Fu, R.E. Cohen, *Nature* 403 (2000) 281.

- [25] Y. Guo, H. Luo, D. Lin, H. Xu, T. He, Z. Yin, *J. Phys.: Condens. Matter* 15 (2003) L77.
- [26] R. Guo, L.E. Cross, S.E. Park, B. Noheda, D.E. Cox, G. Shirane, *Phys. Rev. Lett.* 84 (2000) 5423.
- [27] J.M. Kiat, Y. Uesu, B. Dkhil, M. Matsuda, C. Malibert, G. Calvarin, *Phys. Rev. B* 65 (2002) 064106.
- [28] A.K. Singh, D. Pandey, *Phys. Rev. B* 67 (2003) 064102.
- [29] M. Mahesh Kumar, V.R. Palkara, K. Srinivas, S.V. Suryanarayana, *Appl. Phys. Lett.* 76 (2000) 2764.
- [30] J. Wang, J.B. Neaton, H. Zheng, V. Nagarajan, S.B. Ogale, B. Liu, D. Viehland, V. Vaithyanathan, D.G. Schlom, U.V. Waghmare, N.A. Spaldin, K.M. Rabe, M. Wuttig, R. Ramesh, *Science* 299 (2003) 1719.
- [31] T.P. Comyn, S.P. McBride, A.J. Bell, *Mater. Lett.* 58 (2004) 3844.
- [32] J.R. Cheng, Z.Y. Meng, L.E. Cross, *J. Appl. Phys.* 98 (2005) 084102.
- [33] J.R. Cheng, R. Eitel, L.E. Cross, *J. Am. Ceram. Soc.* 86 (2003) 2111.
- [34] Q.H. Jiang, C.W. Nan, Z.J. Shen, *J. Am. Ceram. Soc.* 89 (2006) 2123.
- [35] J.R. Cheng, Z.Y. Meng, L.E. Cross, *J. Appl. Phys.* 96 (2004) 6611.
- [36] Y.P. Wang, L. Zhou, M.F. Zhang, X.Y. Chen, J.M. Liu, Z.G. Liu, *Appl. Phys. Lett.* 84 (2004) 1731.
- [37] G.L. Yuan, S.W. Or, *Appl. Phys. Lett.* 88 (2006) 062905.
- [38] X.D. Qi, J. Dho, R. Tomov, M.G. Blamire, J.L. MacManus-Driscoll, *Appl. Phys. Lett.* 86 (2005) 062903.
- [39] H. Nagata, N. Koizumi, T. Takenaka, *Key Eng. Mater.* 169/170 (1999) 37.
- [40] G. Shirane, R. Newnham, R. Pepinsky, *Phys. Rev.* 96 (1954) 581.